ANALYSIS OF THE WATER IMPACT OF SYMMETRIC WEDGES WITH A MULTI-MATERIAL EULERIAN FORMULATION

(DOI No: 10.3940/rina.ijme.2012.a4.249)

S Wang and C Guedes Soares. Centre for Marine Technology and Engineering (CENTEC), Instituto Superior Técnico, Technical University of Lisbon, Portugal

SUMMARY

The two-dimensional hydrodynamic problem of a symmetric wedge vertically impacting in calm water is analysed by using an explicit finite element method based on a multi-material Eulerian formulation. The slam-induced loads on wedges with different deadrise angle at a constant velocity are calculated, including pressure distribution, maximum pressure coefficient, force coefficient and time history of vertical force, which are compared with available theoretical and analytical results. The time evolution of pressure distribution and free surface elevation are presented. Furthermore, the effects of impact velocity are investigated. It shows that this method is capable of predicting the local slamming loads, and as well assessing the effects of the deadrise angle and the impact velocity on the slamming pressure for the wedge-shape section.

NOMENCLATURE

β	Deadrise angle (°)
Z_d	Vertical distance from the keel of the Wedge to the calm water (m)
$L(t)$	Half-width of the horizontal wetted surface of the body (m)
S_L	Boundary of the fluid on the left side
S_R	Boundary of the fluid on the right side
S_B	Boundary of the fluid on the bottom
Φ	Potential velocity
η	Water surface (m)
Z	Intersection point between the body and the free surface
n	Unit normal vector to the body surface
v	Rigid body velocity
$\partial/\partial n$	Derivative along the normal vector
ρ	Density of water (kg m^{-3})
p	Pressure (N m^{-2})
p_0	Pressure of atmosphere (N m^{-2})
g	Acceleration of gravity (m s^{-2})
V	Impact velocity (m s^{-1})
F	Total vertical impact force *(N)*
t	Time instance during impact (s)
C_p	Non-dimensional coefficient of pressure
C_{pmax}	Non-dimensional coefficient of the maximum pressure
p_{max}	Maximum pressure (N m^{-2})
C_F	Non-dimensional coefficient of force
B	Half-width of the wedge (m)
$L(t)$	Half-width of the wetted surface (m)
k	pressure coefficient,
$Dw_{rel}(x,t)/Dt$	Impact velocity at the time instance t
a_1, a_3, a_5	Section parameters
ξ	Effective impact angle (°)
k_1	Parameters of the pressure of coefficient
L_{pp}	Ship length (m)
T_d	Period (s)
$\vec{X}$	Lagrangian coordinate
$\vec{x}$	Eulerian coordinate
$\vec{w}$	Relative velocity between the particle velocity and the velocity of the reference coordinate
$\vec{v}$	Fluid particle velocity
$\vec{u}$	Velocity of the reference coordinates
Ω^f	The fluid domain
$\partial\Omega^f$	Boundary of the fluid domain
f	Body force
σ	Total Cauchy stress
μ	Dynamic viscosity
E	The energy of the system
$\partial\Omega_1^f$	The part of the boundary at which the velocity is assumed to be specified
A	Horizontal size of the wedge model (m)
B	Vertical size of the wedge model (m)
C	the length of the wedge model (m)

1. INTRODUCTION

When a high velocity structure impacts with a nearly incompressible fluid, high peak pressures are created. This slam-induced load may lead to local and global damage on a hull structure. The important pioneering study on this subject can be attributed to von Kármàn (1929) who developed an asymptotic theory on the idealized problem of a two-dimensional wedge impacting with a calm water surface, neglecting the local up rise of the water. Based on his work, Wagner (1932) proposed an asymptotic solution for water entry of two-dimensional bodies with small local deadrise angles. This solution was further developed by other researchers (Dobrovol'skaya 1969, Zhao & Faltinsen 1993, 1996).

For the problem of symmetric wedges impacting on the water, there are two different subjects. The water impact

is symmetric when the section enters into the water vertically, while it is asymmetric when the section is inclined or when the water impact has both vertical and horizontal components. In this work, only the first situation is studied. In this case, Dobrovol'skaya (1969) derived an analytical solution by transforming the potential flow problem for the constant water entry of a wedge into a self-similar flow problem in complex plane, which took advantage of the simplicity of the body geometry and is valid for any deadrise angle. Zhao et al. (1993) proposed a nonlinear boundary element method to study the water entry of a two-dimensional body of arbitrary cross-section. In order to verify this solution, they generalized the work of Wagner (1932) and presented a simple asymptotic solution for small deadrise angles, and also derived a similarity solution which was based on the analytical formulation of Dobrovol'skaya (1969). As a further development work, a fully nonlinear numerical simulation method which includes flow separation from knuckles of a body was presented by Zhao and Faltinsen (1996). Motivated by their work, Mei et al. (1999) developed an analytical solution for the general impact problem by adopting the conformal mapping technique.

On the other hand, Stavovy and Chuang (1970) carried out the experimental research on the water entry of rigid and elastic bodies which include rigid flat and rigid wedges with deadrise angles of 1°, 3°, 6°, 10° and 15°, and obtained the relationship between maximum pressure and deadrise angle. Ochi and Motter (1973) obtained the slamming loads in terms of slamming pressure, the pressure distribution and the time variation of the total slamming load by analysing many test results. More recently, a drop test for a wedge with deadrise angle 30° was carried out by Zhao et al. (1996) in MARINTEK. Brizzolara et al. (2008) predicted the impact pressures and slamming forces for a bow section using a range of two-dimensional potential and viscous flow method, and compared with experimental measurements.

Recently, the finite element method is widely used in the full coupled problems of fluid-structure interaction. Kihara (2004) proposed two computational model of the jet flow to investigate the water entry problems of a wedge, however, only the results for deadrise angle 30º and 60º are validated Peseux et al. (2005) studied the three-dimensional water impact of rigid and flexible bodies by using the finite element method and experimental solution, but their simulations are only conducted for three cones. Stenius et al. (2006) examined the ability of the explicit finite element method to study the fluid-structure interaction problem. Das and Batra (2011) studied delamination induced in a sandwich composite panel due to the hydroelastic pressure by using the coupled Lagrangian and Eulerian formulation.

In this work, an explicit finite element method, based on a multi-material Eulerian formulation and a penalty coupling algorithm, is applied to evaluate the slam-induced loads on symmetric wedges with various deadrise angles varying from 10º to 60º. This method has been verified by author's previous work in Luo et al. (2011) and Wang et al. (2012) on water entry problems by comparing the predictions with the available experimental measurements from Zhao and Faltinsen (1996). For further study, the effects of deadrise angle are discussed here, according to the calculations in terms of maximum value of pressure, pressure distribution, non-dimensional vertical impact force, and the time history of impact force. Finally the predictions in this work are compared with available numerical and analytical results. Furthermore, the effects of impact velocity are also studied. The agreements between the present predictions and other calculations are good, and the computational time required is acceptable as well.

2. METHODS

2.1 THEORETICAL BACKGROUND

A symmetric water entry of a two-dimensional wedge is shown in Figure 1. The deadrise angle is denoted as β. A Cartesian coordinate system *(y, z)* is introduced, and the *y*-axis is placed in the undisturbed water surface, while the *z*-axis is located in the symmetric line of the wedge. The wedge enters the calm water with a vertical velocity which is denoted as *dz/dt*. During the water entry, Z_d indicates the vertical distance from the lowest point to the calm water, and *L(t)* represents the half-width of the horizontal wetted surface of the body. The boundaries of the water are denoted as S_L, S_R and S_B.

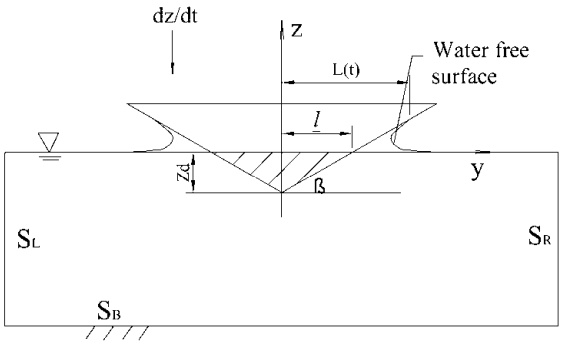

Figure 1. Symmetric water entry of a two-dimensional wedge.

The fluid is assumed to be incompressible and the flow irrotational and no air pocket is created during the impact, so that the velocity potential Φ which describes the water flow satisfies the Laplace equation,

$$\frac{\partial^2 \phi}{\partial y^2} + \frac{\partial^2 \phi}{\partial z^2} = 0 \qquad (1)$$

The kinematic free surface boundary condition is written as

$$\frac{D\phi}{Dt} = \frac{\partial \phi}{\partial z} \qquad \text{on } z = \eta(y,t) \tag{2}$$

The dynamic free surface boundary condition can be written as

$$\frac{D\phi}{Dt} = \frac{1}{2}\left[\left(\frac{\partial \phi}{\partial y}\right)^2 + \left(\frac{\partial \phi}{\partial z}\right)^2\right] - gz \qquad \text{on } z = \eta(y,t) \tag{3}$$

Wagner (1932) developed an asymptotic solution for the water entry of two-dimensional bodies with small local deadrise angles, neglecting the gravity. He simplified the dynamic boundary condition in the outer flow domain as $\Phi=0$ which was applied on the horizontal line that starts at the intersection point between the body and the free surface. The kinematic free surface condition was used to determine the intersection between the free surface and the body in the outer flow domain. The linearized kinematic free surface boundary condition is:

$$\frac{\partial \eta}{\partial t} = \frac{\partial \phi}{\partial z}, \text{ on } Z = \eta(Y,t) \tag{4}$$

where $Z=\eta(Y, t)$ means the intersection point between the body and the free surface. The linearized dynamic free surface boundary condition is:

$$\phi = 0, \text{ on } Z = \eta(Y,t) \tag{5}$$

The kinematic body boundary condition is:

$$\frac{\partial \phi}{\partial n} = -vn_z \text{ on the body surface} \tag{6}$$

where $n=(n_y, n_z)$ is the unit normal vector to the body surface, v is the rigid body velocity and $\partial/\partial n$ is the derivative along the normal vector. The positive direction of n is into the fluid domain. After obtaining the velocity potential function based on the initial conditions and far-field condition, the pressure on the body p can be calculated using Bernoulli's equation:

$$\frac{p - p_0}{\rho} = -\frac{\partial \phi}{\partial t} - \frac{1}{2}\left[\left(\frac{\partial \phi}{\partial y}\right)^2 + \left(\frac{\partial \phi}{\partial z}\right)^2\right] \tag{7}$$

Dobrovol'skaya (1969) and Zhao and Faltinsen (1993) presented similarity solutions for wedges by using Wagner's h-function. Zhao and Faltinsen (1993) also proposed a fully nonlinear boundary element method which ignored the contributions of the thin jet of water to the total force on the body, considering that the pressure of this part is close to the atmospheric pressure, and applied the exact body boundary condition. This method was further developed in Zhao and Faltinsen (1996) which extended it to general asymmetric bodies.

A simplified solution was also presented by Zhao and Faltinsen (1996) based on the Wagner's asymptotic solution. The wetted body surface was found by integrating in time the vertical velocity of fluid particles on the free surface and finding when the particles intersect the body surface. The main difference from Wagner's solutions is that the exact body boundary was applied at each time instance, while Wagner (1932) used the simplified body boundary condition.

In this work, the available calculations from the methods mentioned above are used to compare with the simulated results from LS-DYNA, together with the analytical calculations from Ochi and Motter (1973), Stavovy and Chuang (1976) and Mei et al. (1998) who obtained the empirical or analytical formulations by means of experiments or analytical solutions.

2.2 ANALYTICAL FORMULATIONS

2.2(a) Maximum coefficient of pressure

The maximum value of the pressure coefficient is:

$$C_p = \frac{p_{\max} - p_0}{\frac{1}{2}\rho V^2} \tag{8}$$

Assuming that the wedge enters into water with a constant velocity, the peak value of pressure coefficient is obtained by Wagner (1932):

$$C_{p\max} = 1 + \frac{\pi^2}{4\tan^2\beta} \tag{9}$$

On the other hand, the theorem of impulse assumes that the maximum impact pressure is proportional to the quadratic impact velocity, as:

$$P_{\max}(x) = \frac{1}{2}\rho k\left|\frac{Dw_{rel}(x,t)}{Dt}\right|^2 \tag{10}$$

where k represents the pressure coefficient, and $Dw_{rel}(x,t)/Dt$ is the impact velocity at the time instance t. The k value can be evaluated for any section by Ochi and Motter (1973), which is expressed as follows:

$$k = \exp(1.377 + 2.419a_1 - 0.873a_3 + 9.624a_5) \tag{11}$$

where, a_1, a_3, a_5 were calculated based on mapping of the section for any conventional hull shape below 1/10 of the design draft waterline into a circle. Stavovy and Chuang (1976) proposed an empirical formulation for the pressure coefficient obtained from a large amount of experiments as follows:

$$k = 288k_1 / \cos^4 \xi(x,t) \tag{12}$$

where $\cos\xi(x,t)$ is the effective impact angle, and k_1 is expressed using a series of polynomials that fit the experimental results as:

$$k_1 = \begin{cases} = 0.37\xi/2.2 + 0.5, 0 \le \xi < 2.2^\circ \ldots\ldots\ldots\ldots\ldots\ldots\ldots\ldots\ldots\ldots \\ = 2.1820894 - 0.9451815\xi + 0.203754\xi^2 - 0.0233896\xi^3 \\ + 0.0013578\xi^4 - 0.00003132\xi^5, 2.2^\circ \le \xi < 11^\circ \\ = 4.748742 - 1.3450284\xi + 0.1576516\xi^2 - 0.0092976\xi^3 \\ + 0.0002735\xi^4 - 0.00000319864\xi^5, 11^\circ \le \xi < 20^\circ \\ = (1 + 2.4674/\tan^2 \xi)0.76856471/288, 20^\circ \le \xi \ldots\ldots\ldots\ldots\ldots \end{cases} \tag{13}$$

2.2(b) Vertical impact force

By integrating the equation of the pressure along the surface of the body, the vertical slamming force was given by Wagner (1932) as:

$$\begin{aligned} F &= \int_{-L}^{L} p dy = \rho V L \frac{dL}{dt} \int_{-L}^{L} \frac{dy}{\sqrt{L^2 - y^2}} + \rho \frac{dV}{dt} \int_{-L}^{L} \sqrt{L^2 - y^2}\, dy \\ &= \rho \pi V L \frac{dL}{dt} + \rho \frac{\pi}{2} L^2 \frac{dV}{dt} \end{aligned} \tag{14}$$

For a wedge,

$$L(t) = \frac{\pi}{2\tan\beta} \int_0^t V(\tau) d\tau \tag{15}$$

The vertical force coefficient for a unit length wedge with constant velocity during water entry is

$$C_F = \frac{F}{\rho V^3 t} \tan^2 \beta \tag{16}$$

So, for Wagner's model, the vertical force coefficient is equal to *3π/4*. Due to neglecting the free surface elevation, the vertical force coefficient of von Kármàn's model is equal to π.

Based on equation (16), Zhao and Faltinsen (1996) compared the total force on a wedge with different deadrise angles by using the methods of von Kármàn (1929), Wagner (1932), von Kármàn-moment which is obtained by using the exact body boundary condition and the principle of conservation of momentum, the simplified solution and the similarity solution.

In Zhao and Faltinsen (1993) the pressure distribution on the wedge has a sharp value in a *z*-position, according to the asymptotic theory, equal to *(0.5 π-1) z_d* . Based on the direct integration of the pressure, they gave the values of the total non-dimensional vertical force as:

$$F_{AD} = \frac{F}{\rho v^2 z_d} \tag{17}$$

when the impact velocity is constant, zd is equal to vt.

For the time history of the vertical slamming force, Ochi & Motter (1973) proposed a simple form to evaluate the time variation of the vertical slamming force. They assumed that the time history had a triangular varying from 0 to the maximum value and to 0 again during a period T_d. According to experimental work and Froude scale law, the relationship between the period and the ship length was given as:

$$T_d = 0.00794\sqrt{L_{pp}} \tag{18}$$

where L_{pp} is the ship length.

Mei et al. (1999) developed an analytical solution for the general impact problem by adopting the assumptions of Zhao and Faltinsen (1996) and the conformal mapping technique.

2.3 EXPLICIT FINITE ELEMENT METHOD

The explicit finite element method LS-DYNA is used in this work to predict the slamming loads on the surface of symmetric wedges with different deadrise angles. The FEM is based on a Multi-Material Arbitrary Lagrangian Eulerian (MMALE) formulation and a penalty coupling method. For single material or multi-material Eulerian formulation, the mesh is fixed in space and materials flow through the mesh using an advection scheme to update fluid velocity and history variables. This takes away all problems associated with distorted mesh that are commonly encountered with a Lagrangian or Arbitrary-Lagrangian-Eulerian (ALE) formulation. Therefore, Aquelet et al. (2005) concluded that the Euler Lagrange coupling using Eulerian multi-material formulation for the fluid is more suitable for solving slamming problems.

2.3(a) Governing equations for fluids and structure

In Arbitrary Lagrangian-Eulerian (ALE) formulation, a reference coordinate which is not the Lagrangian coordinate and Eulerian coordinate is induced. The differential quotient for material with respect to the reference coordinate is described as following equation:

$$\frac{\partial f(\vec{X}, t)}{\partial t} = \frac{\partial f(\vec{x}, t)}{\partial t} + \vec{w} \frac{\partial f(\vec{x}, t)}{\partial x} \tag{19}$$

where, $\vec{X}$ is Lagrangian coordinate, $\vec{x}$ is Eulerian coordinate, and $\vec{w}$ is relative velocity between the particle velocity $\vec{v}$ and the velocity of the reference coordinate $\vec{u}$. Therefore, the Arbitrary Lagrangian-

Eulerian formulation can be derived from the relation between the time derivative of material and that of reference geometry configuration.

Let $\Omega^f \in R^3$ represent the fluid domain, and $\partial\Omega^f$ denote its boundary. The equation of mass, momentum and energy conservation for a Newtonian fluid in ALE formulation in the reference domain, are given by:

$$\frac{\partial \rho}{\partial t} = -\rho div\left(\vec{w}\right) - \vec{w} \cdot grad(\rho) \tag{20}$$

$$\sigma \frac{\partial \vec{v}}{\partial t} = \overrightarrow{div}\left(\overline{\overline{\sigma}}\right) + \vec{f} - \rho \vec{w} \cdot \overline{\overline{grad}}\left(\vec{v}\right) \tag{21}$$

$$\rho \frac{\partial E}{\partial t} = \overline{\overline{\sigma}} : \overline{\overline{grad}}\left(\vec{v}\right) + \vec{f} \cdot \vec{v} - \rho \vec{w} \cdot \overrightarrow{grad}(E) \tag{22}$$

where ρ is the fluid density, f is the body force and σ is the total Cauchy stress given by:

$$\overline{\overline{\sigma}} = -p \cdot \overline{\overline{Id}} + \mu\left(\overrightarrow{grad}(v) + \left(\overrightarrow{grad}(v)\right)^T\right) \tag{23}$$

where p is the pressure and μ is the dynamic viscosity. The part of the boundary at which the velocity is assumed to be specified is denoted by $\partial\Omega_1^f$, the inflow boundary condition is:

$$\vec{v} = \vec{g}(t) \text{ on } \partial\Omega_1^f \tag{24}$$

The traction boundary condition associated with equation (21) is the conditions on stress components. These conditions are assumed to be imposed on the remaining part of the boundary:

$$\overline{\overline{\sigma}} \cdot \vec{n} = \vec{h}(t) \text{ on } \partial\Omega_h \tag{25}$$

The Multi-Material Eulerian formulation is part of the Arbitrary-Lagrangian-Eulerian (ALE) solver, which involves a Lagrangian step, where the mesh is allowed to move and a second step that advects the element state variables back onto a reference mesh. The multi-material Eulerian formulation is a specific ALE case where the reference mesh velocity is zero, which means:

$$\vec{u} = 0 \tag{26}$$

Let $\Omega^s \in R^3$, the domain occupied by the structure, and let $\partial\Omega^s$ denote its boundary. A Lagrangian formulation is considered, so the movement of the structure Ω^s described by $x_i(t)(i = 1,2,3)$ can be expressed in terms of the reference coordinates $X_\alpha(\alpha = 1,2,3)$ and time t

$$x_i = x_i\left(X_\varepsilon, t\right) \tag{27}$$

The momentum equation is given by:

$$\rho \frac{d\vec{v}}{dt} = \overrightarrow{div}\left(\overline{\overline{\sigma}}\right) + \vec{f} \tag{28}$$

where ρ is the fluid density, f is the force density and σ is the total Cauchy stress. The solution of equation (28) satisfies the displacement boundary condition equation (29) on the boundary $\partial\Omega_1^s$ and the traction boundary condition equation (30) in the boundary $\partial\Omega_2^s$.

$$\vec{x}\left(\vec{X}, t\right) = \vec{D}(t) \text{ on } \partial\Omega_1^s \tag{29}$$

$$\overline{\overline{\sigma}} \cdot \vec{n} = \vec{\tau}(t) \quad \text{on } \partial\Omega_2^s \tag{30}$$

where $\vec{n}$ is the unit normal oriented outward at the boundary $\partial\Omega^s$, $\vec{D}(t)$ is the displacement vector and $\vec{\tau}(t)$ is the traction vector.

2.3(b) Euler-Lagrange coupling

The governing equations of fluid domain and structure domain are presented above. To activate the interaction between the fluid and the structure, an Euler-Lagrange coupling method is introduced. Euler-Lagrange coupling allows the treatment of the impact problems involving fluids because this coupling treats the interaction between a Lagrangian formulation modelling the structure and an Eulerian formulation modelling the fluid. In addition, an algorithm is needed to make the structure and fluid interact.

The penalty coupling algorithm is applied in this work. It is designed to preserve the total energy of the system as well as possible. The constrained based method consumes some kinetic energy, which is a problem in many applications. Penalty coupling behaves like a spring system and penalty forces are calculated proportionally to the penetration depth and spring stiffness. The stiffness of the spring is given in term of the bulk modulus of the fluid element in the coupling containing the slave structure node, the volume of the fluid element that contains the master fluid node, and the average area of the structure elements connected to the structure node. However, to avoid numerical instabilities, a penalty factor is introduced for scaling the estimated stiffness of the interacting (coupling) system. For impact problems, we always have to examine the influence of this parameter on the solution (Aquelet et al. 2005). For the problem of two-dimensional wedge, Luo et al. (2011) conducted the parameters study, including the penalty factor, time step factor, mesh size and the number of the contact points, and validated this method by comparing the predictions with the experimental results from Zhao and Faltinsen (1996). The results show that mesh size is of great importance for the simulations, while other aspects affect little.

3. FE-MODELING

In this work, the fluid is solved by using an Eulerian formulation, while the wedge is discretized by a Lagrangian approach. The fluids (water and air) are defined as the multi-material group, which means that the effects of the water and the air are all considered.

This work focus on the predicted impact loads on symmetric wedges with different deadrise angles, so the model setup is not included, however, it can be found in Luo et al. (2011). The gravity effects are discussed in Wang (2012) which shows that they can be neglected here. The impact velocity is assumed constant in present work. Unless otherwise specified, the impact velocity is -6.15 m/s in the *z*-direction.

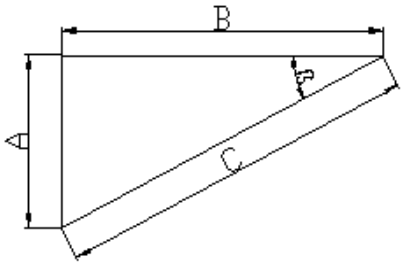

Figure 2. The geometry of the wedge used in the calculations.

Due to the symmetric property of the section, only half of the system is modelled, as shown in Figure 2. The geometry of the wedge is varying with the deadrise angle β. Accordingly, the sizes of the wedges with different deadrise angle are listed in Table 1. Furthermore, the length of the section in *x*-direction is 2.5mm for all cases, which means the mesh size of the model is 2.5mm based on the two-dimensionality of the simulation. The mass of the section is 0.326kg.

Table 1. Parameters of the symmetric wedges.

β(°)	A(m)	B(m)	C(m)
10	0.044	0.25	0.254
15	0.067	0.25	0.259
20	0.091	0.25	0.266
25	0.117	0.25	0.276
30	0.1443	0.25	0.289
40	0.2098	0.25	0.326
45	0.2500	0.25	0.354
60	0.1732	0.10	0.200

4. RESULTS AND DISCUSSION

4.1 PRESSURE DISTRIBUTION

The simulated pressure distributions on the wetted surfaces of the wedges with different deadrise angle varying from 10° to 60° are presented in Figure 3, in which the published results from Dorbrovol'skaya (1969), Zhao and Faltinsen (1993, 1996) and Mei et al. (1998) are included as well. The results from the asymptotic formulation of Zhao and Faltinsen (1993) are only available for the deadrise angle smaller than 30°. For the predictions of LS-DYNA, the pressure distribution for a wedge is varying from one time instant to another. Corresponding to the analytical results, the plotted ones are the pressure distributions at the time when the pressures come up to peak values.

For the variables of these figures, z_d is the vertical distance from the bottom surface of the wedge to the keel, and means the draft of the section, thus 0 represents the intersection between the section and the undisturbed water and -1 means the keel of the body. C_p is a non-dimensional coefficient of the pressure.

When the deadrise angle is small, the predicted results are in good agreement with the numerical and analytical calculations in the initial stage of the water impact; however, the simulated peak values of the pressure are much smaller in the later stage. As the deadrise angle increases, the agreement in the later stage between LS-DYNA and other solutions are more satisfactory, in particular for the cases of 30° and 40°.

When the deadrise angle is 60°, they have good agreement except that the simulated pressure on the position near the keel of the wedge is smaller than other predictions. For the results of Mei et al. (1998), the pressure drops fast after coming up to the peak value, which means that the free surface elevation was not considered.

Though there are some differences between these solutions, the same conclusion can be obtained from the calculations. When the deadrise angle is small, the maximum pressure is located near the spray root of the water jet, and the pressure is approximately uniformly distributed along the wetted surface when the deadrise angle is close to 45°, while it moves to the keel of the wedge for larger deadrise angles.

For the pressure distribution, it is observed that the predictions at later stage in present work are much smaller than other calculations when the deadrise angle is small. Probably, this is because the water jet reaches the domain where the mesh size is not fine enough at the late stage. For a smaller deadrise angle, the water jet goes farther toward the boundary. This can be observed in the evolution of water surface elevation.

Furthermore, the positions of maximum pressures for different deadrise angles, which are defined as the ratio between the z-coordinate of the position of the maximum pressure and the penetration of the body underwater, are plotted in Figure 4. Z_{max} means the z-coordinate of the bottom surface in which the maximum pressure located. As seen in Figure 4, as the deadrise angle increases, the position becomes lower. The predictions for small

deadrise angles from LS-DYNA are lower than other calculations, while they are in good agreement when the deadrise angle is close to 30º and over. When the deadrise angle is larger than 40º, the position of maximum pressure is located near the keel.

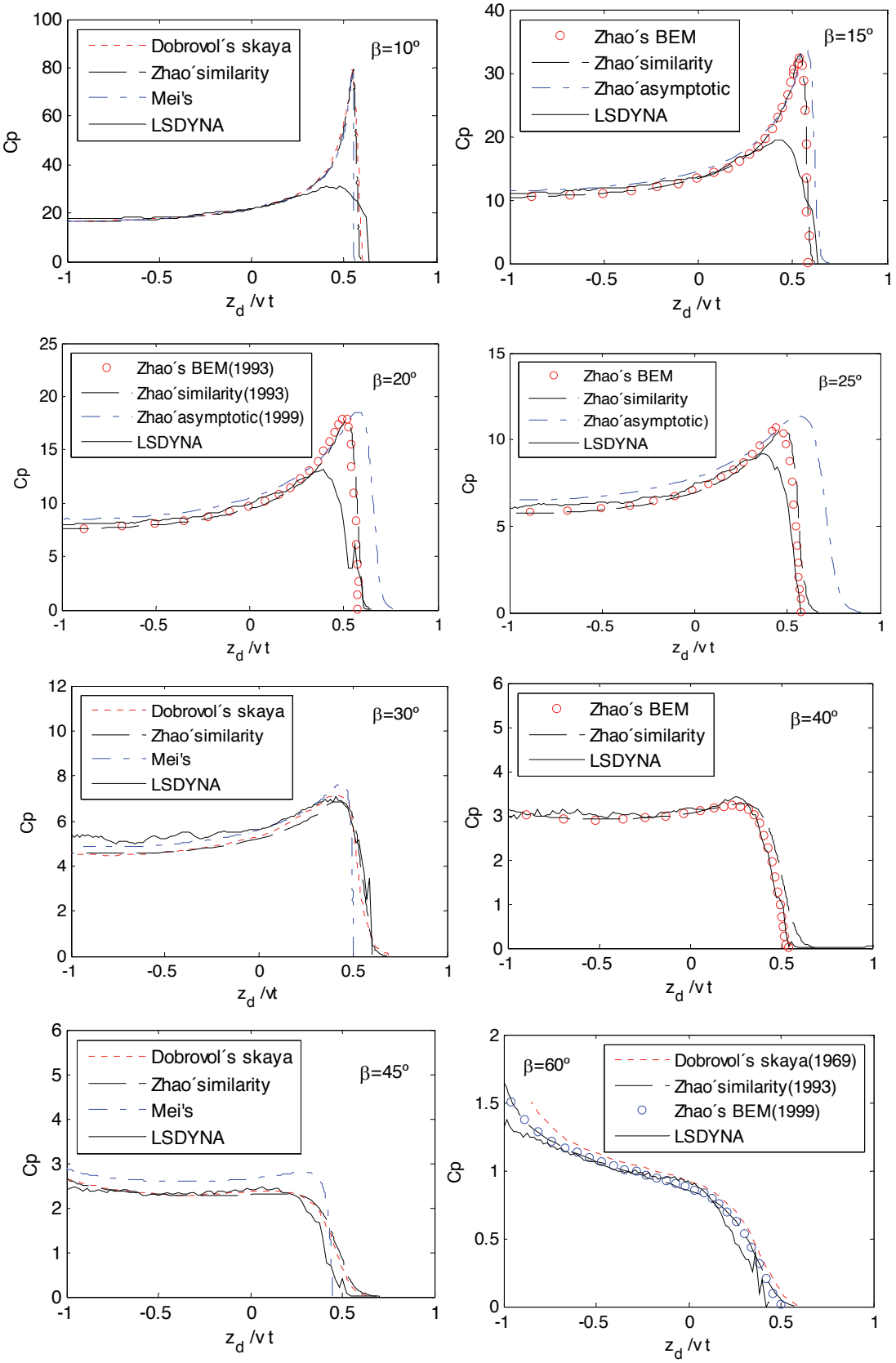

Figure 3. Pressure distributions on symmetric wedges with constant impact velocity for different deadrise angles.

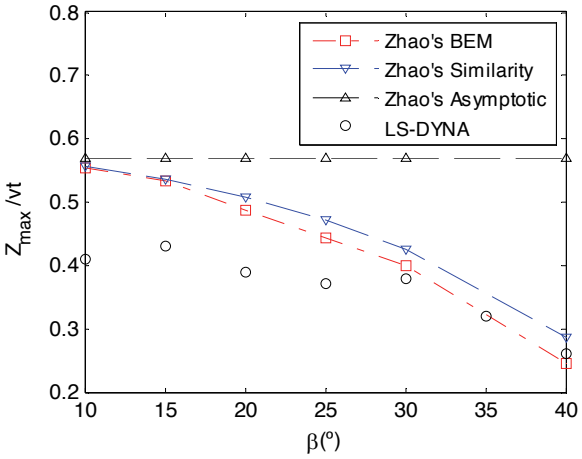

Figure 4. Position of maximum pressure.

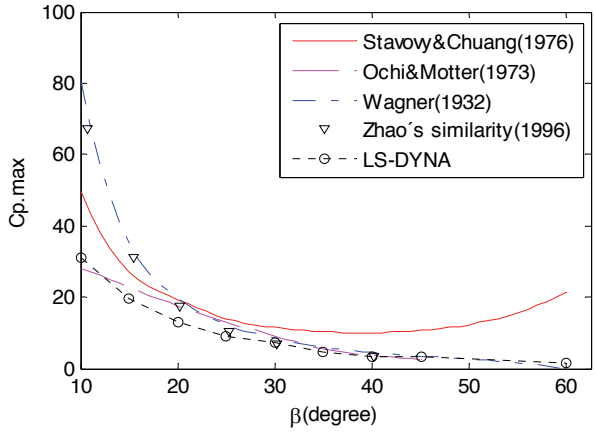

Figure 5. Maximum coefficients of pressure on symmetric wedges with constant impact velocity for different deadrise angles.

4.2 MAXIMUM COEFFICIENT OF PRESSURE

The maximum pressure coefficients are computed for the deadrise angle varying from 10° to 45°. Figure 5 shows the comparisons of the maximum coefficients of pressure on the wetted surface of wedges with different deadrise angles. It shows that the smaller is the deadrise angle, the larger is the pressure coefficient. This was noticed previously by several researchers such as Dobrovolskaya (1969), Zhao and Faltinsen (1993) and Mei et al. (1999).

As plotted in Figure 5, when the deadrise angle is small, the predicted values are much smaller than the results from Wagner's (1932), Stavovy and Chuang's (1976) and Zhao's similarity (1996) solution, while they are closer to the results from Ochi and Motter (1973).

When the deadrise is larger, the predictions agree well with the results from the three analytical methods, however, the values are a little smaller than those from Chuang's formulation. In general, the predictions of maximum pressure from LS-DYNA are of best agreement with the values of Ochi and Motter (1973).

4.3 NON-DIMENSIONAL COEFFICIENT OF IMPACT FORCE

Figure 6 plotted the non-dimensional coefficients of impact force for different deadrise angles, based on the definition of equation (18). It shows that the simulated results by LS-DYNA are in good agreement with the predictions obtained by using Zhao and Faltinsen (1996)'s BEM, while they are much larger than those from Ochi and Motter (1973). It is because that Ochi and Motter (1973) assumed that the slamming pressure has a linear distribution vertically with the maximum value at the bottom and the zero value at one tenth of the design draft, and the total vertical force is obtained by integrating the pressure along the hull. For the Stavovy and Chuang (1976)'s work, the pressure in a wedge was assumed constant and the vertical force was obtained by multiplying the maximum pressure with the horizontal size of the wedge, so the total impact force was overestimated. As shown in Figure 6, the coefficients of the impact force calculated in present work are much smaller than those from Stavovy and Chuang (1976).

Ramos and Guedes Soares (1998) represented the predicted non-dimensional vertical force for a rigid wedge with different deadrise angles. They applied the pressure distribution obtained using the Stavovy and Chuang (1976)'s method to their proposed method for the evaluation of the vertical transient load, because of the simplicity and the limited computer effort of this solution. Nevertheless, as plotted in Figure 5 and Figure 6, the pressure and the slamming force calculated by Stavovy and Chuang (1976) are obviously over predicted for a large deadrise angle.

On the other hand, the vertical force coefficient for a unit length wedge with constant velocity during water entry is given by equation (16). Based on this equation, the numerically simulated results are plotted in Figure 7, together with the analytical values.

The Wagner (1932) solution clearly overestimates the slamming force for large deadrise angles, while the two different von Kármàn solutions, one of which is based on a flat plate solution and the other one is obtained by using the exact body boundary condition and the principle of conservation of momentum, underestimate the slamming force for small deadrise angles.

There are good agreement between the simplified and the similarity solution proposed by Zhao and Faltinsen (1996). The simulated values by LS-DYNA are between the results of Zhao and Faltinsen and von Kármàn when the deadrise angle is smaller than 60°. For the deadrise angle around 45°, the simulated predictions have good agreement with those from von Kármàn. Furthermore, the vertical slamming force for the 15° deadrise angle is larger than the one for the 10°, which may be due to the numerical noise of the results.

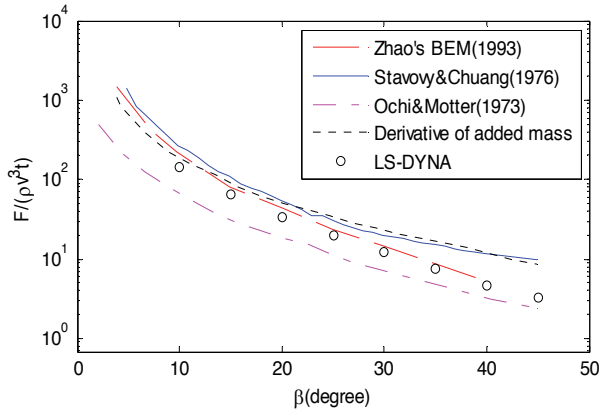

Figure 6. Non-dimensional coefficients of impact force on symmetric wedges with constant impact velocity for different deadrise angles.

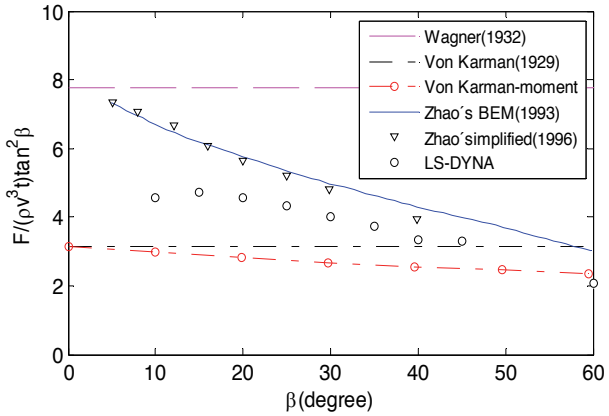

Figure 7. Comparison of the predictions of coefficient of vertical slamming force.

4.4 TIME HISTORY OF THE IMPACT FORCE

As mentioned before, Ochi and Motter (1973) proposed a simple form to evaluate the time variation of the vertical slamming force. They assumed that the time history had a triangular varying from 0 to the maximum value and to 0 again during a period T_d

In order to compare the predicted vertical force with the simple form, assume that the length of the ship is L_{pp}, and the maximum value occurs at the time instance of $T_d/2$. Since the maximum slamming force of the simple form from Ochi and Motter (1973) is normalized to 1, the one from LS-DYNA can be calculated using the same method. For different deadrise angles of the wedge, the time histories of the vertical slamming force are distinct. The simulated vertical forces can be obtained by integrating the pressure on the wetted surface of symmetric sections at each time instance. The predicted time histories of the vertical slamming force for the wedges with deadrise angle of 15°, 30° and 45°, are shown in Figure 8, which show that the slamming force from LS-DYNA is almost linearly related to time during the first period of $T_d/2$ as same as the simple form, however it does not drop to zero during the period. In the later stage of the impact, the predicted vertical force drops fast due to the flow separation, and then decreases gradually.

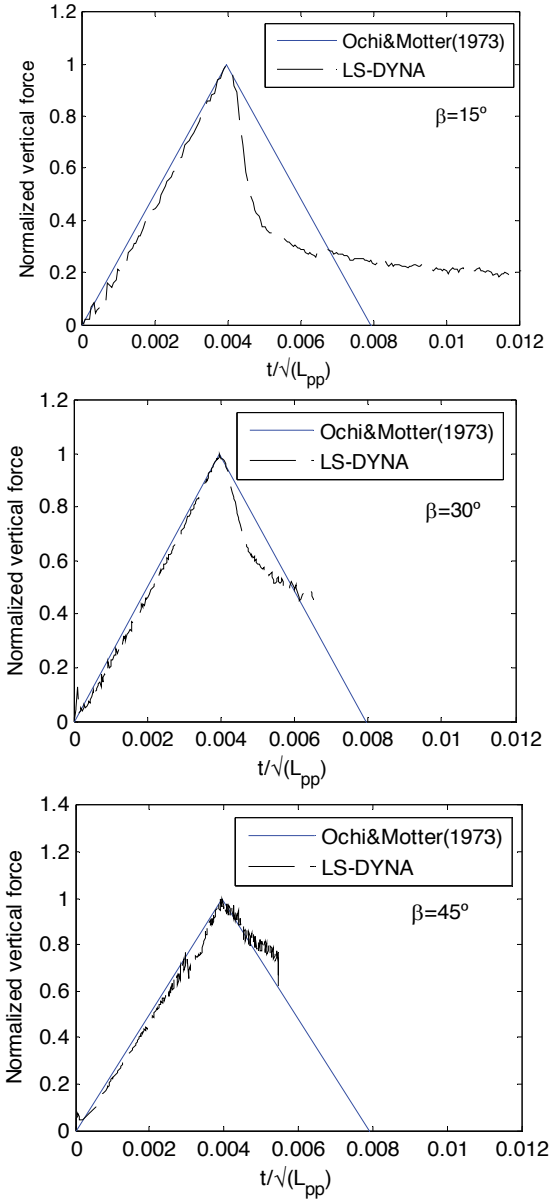

Figure 8. Comparison of time history of vertical force between LS-DYNA and Ochi and Motter (1973)'s simple form.

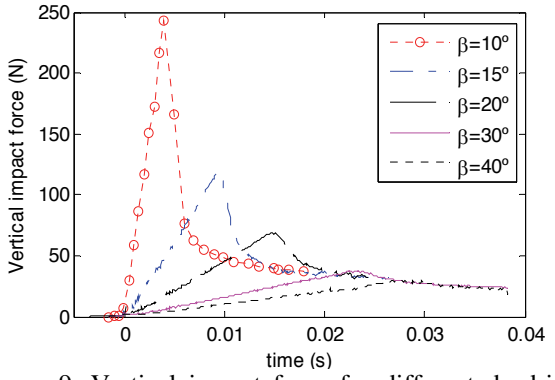

Figure 9. Vertical impact force for different deadrise angles.

Figure 9 shows the simulated vertical impact force for wedges with deadrise angle varying from 10° to 40°. It can be found that the maximum value of the vertical force becomes larger as the deadrise angle decreases. As listed in Table 1, the vertical size of the wedge is larger for a larger deadrise angle, so the maximum value occurs later when the deadrise angle is larger as shown in Figure 9.

At the later stage of the impact, the vertical impact force reduces quickly after flow separation and then decays more slowly towards to a value which is similar for all the deadrise angles.

4.5 PRESSURE DISTRIBUTION AND FREE SURFACE ELEVATIOV AT DIFFERENT TIME INSTANCES

Figure 10 shows the pressure distributions at different time instances for the cases of β=15°, β=45°and β=60°. Accordingly, the evolutions of the free surface elevations are presented in Figure 11, which also illustrates the pressures on the wetted surface of the wedges in terms of the pressure contours. For the variables in Figure 10, y/B means the relative position of the points on the surface of section, where y is the horizontal coordinate of the bottom surface and B is the half-width of the section. 0 s means the time instance when the section touches the water.

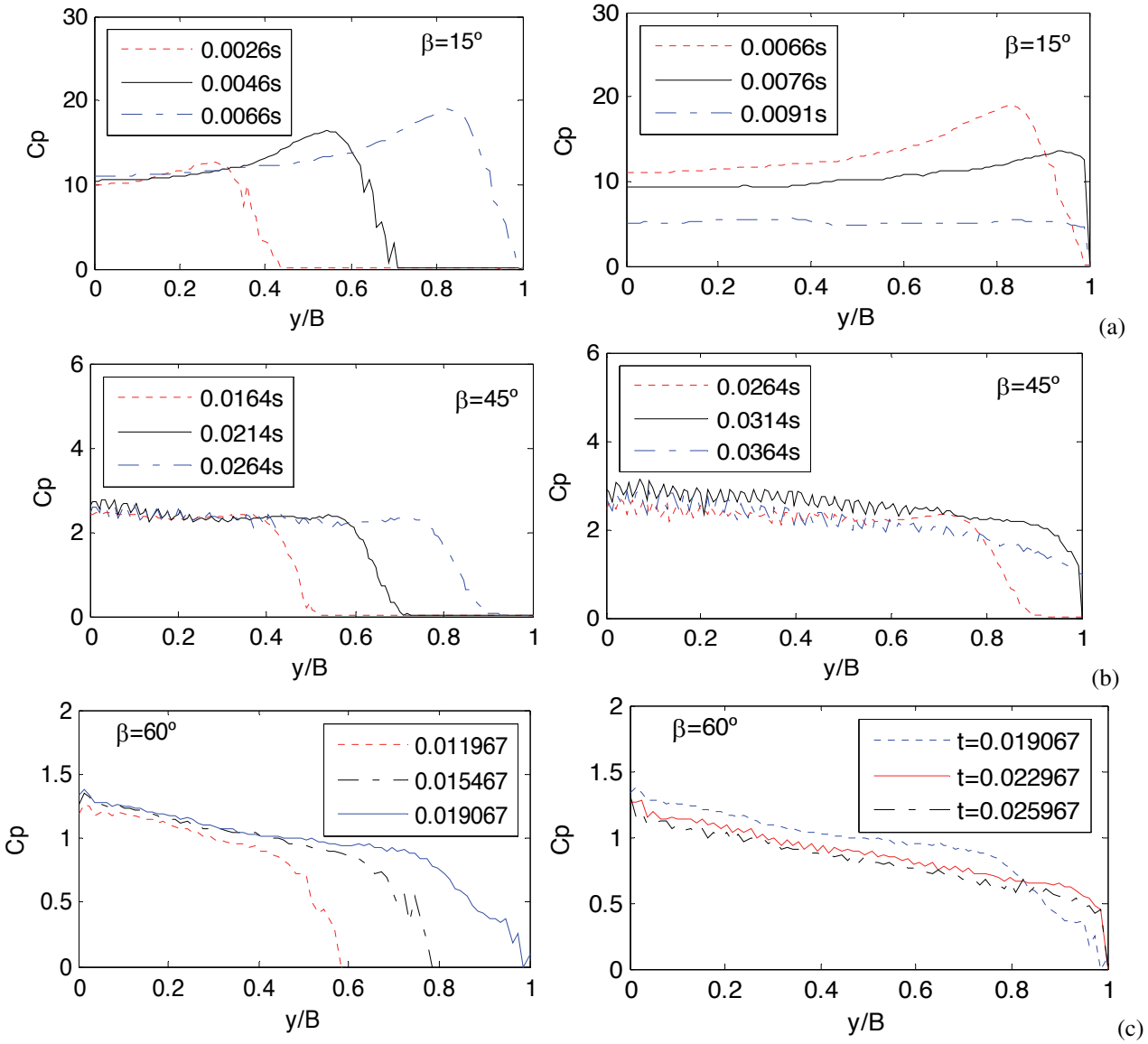

Figure 10. Evolution of the pressure distribution for different deadrise angles.

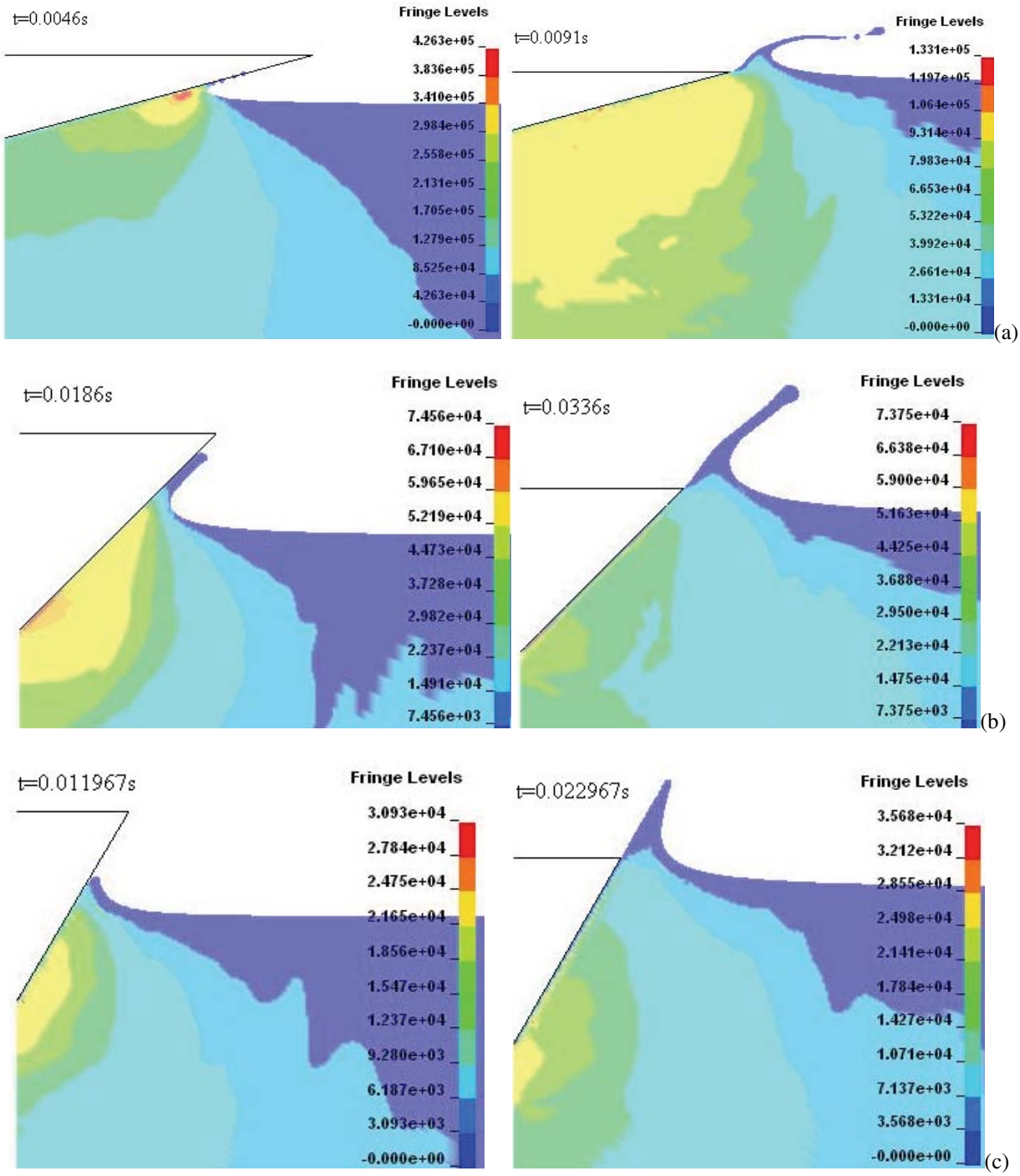

Figure 11. Evolution of the free surface elevation for different deadrise angles. (a) $\beta = 15^{\circ}$, (b) $\beta = 45^{\circ}$, (c) $\beta = 60^{\circ}$.

When the deadrise angle is 45º, the pressure is distributed on almost the whole wetted surface of the section before flow separation; however, the maximum pressure is located near the keel and the pressure distribution at different time instants do not change too much. After flow separation, the pressure near the highest position decreases much, while the values at the keel do not change too much. When the deadrise angle is 60º, the maximum pressure is located at the keel of the wedge during the entire water impact as seen in Figure 10(c) and Figure 11(c).

As plotted in Figure 11(a), when the deadrise angle is 15º, a water jet evolves from the free surface at t=0.0046s, meanwhile the maximum pressure is located near the spray root of the water jet as shown in Figure 11(a). After flow separation, e.g., at t=0.0076s, the pressures on the bottom reduce, in particular the ones near the highest positions, and the maximum pressure moves towards the keel of the section.

4.6 EFFECTS OF THE IMPACT VELOCITY

Different impact velocities which include 1m/s, 2m/s, 3m/s, 4m/s, 5m/s and 6.15m/s, are applied for the rigid wedges with the deadrise angles of 15°, 30°, 45° and 60°. The predicted maximum pressure on the wetted surface of wedges with different impact velocities are compared with the published analytical results in Figure 12.

As plotted in Figure 12, the maximum pressures increase with the increasing impact velocity, and also increase with the decreasing deadrise angle when the impact velocity is the same. When the deadrise angle is 15°, the analytical values from Stavovy and Chuang (1976) are much larger than the simulated ones, while the results of Wagner (1932) are the smallest. As to the values from Ochi and Motter (1973), the differences between them and the predicted ones from LS-DYNA become larger when the impact velocity is larger.

When the deadrise angle is 30°, the predictions from LS-DYNA are the smallest compared to other analytical ones, while those of Stavovy and Chuang (1976) are the largest and the other two methods almost have the same results, especially when the impact velocity is small.

The analytical method of Stavovy and Chuang (1976) significantly overestimates the maximum pressure when the deadrise angle is 45° and 60°, and the results from Wagner (1932) are somehow larger than those from LS-DYNA when the impact velocity is larger than 3m/s. Actually, it can be found in Figure 5, that the maximum pressure coefficient calculated by Stavovy and Chuang (1976) are much larger than that from other methods when the deadrise angle is larger than 30°.

5. INFLUENCE OF MODELLING

In present work, in order to compare the predictions with other theoretical and analytical results, the impact velocity is assumed constant in the simulations. In reality, the water entry velocity is varying due to the impact force. Here, the effects of the constant velocity are examined in terms of the pressure histories on the wetted surface of the wedges. For the Euler-Lagrange coupling algorithm, the contact stiffness between the master and slave node has been of much concern. The related parameters used in this work are presented in this section. Another important factor is the computational time. The associated parameters and the total computational time are also stated here.

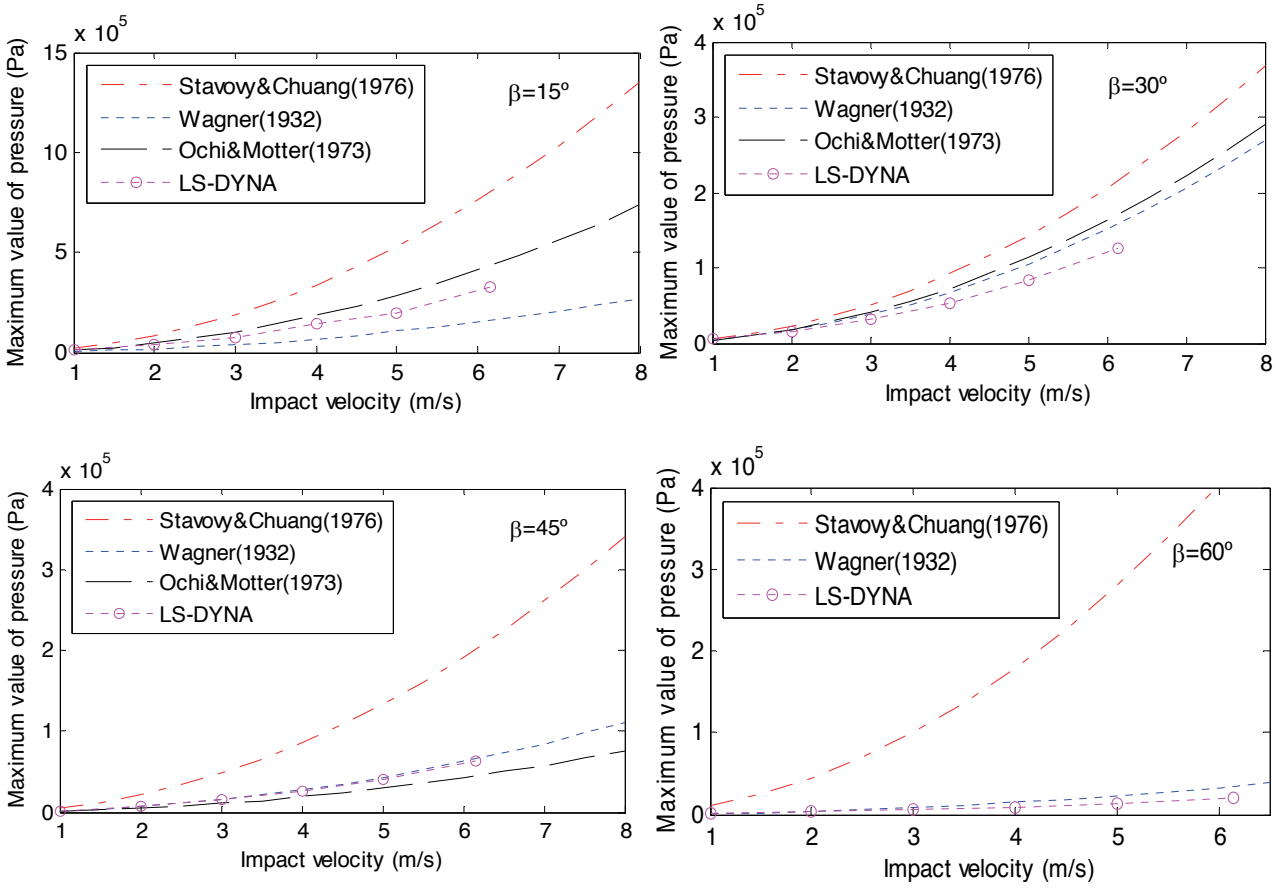

Figure 12. Maximum values of pressures for different impact velocity when the deadrise angle is 15°, 30° and 60°.

5.1 EFFECTS OF THE CONSTANT VELOCITY

As mentioned before, the impact velocity is assumed constant in this work, in order to compare the predictions with the available theoretical and analytical results. To examine the effects of the constant velocity, the pressure histories on the wedges of deadrise angles 15º, 30º, 45º and 60º are presented in Figure 13. Three locations on *y=0.25B, y=0.5B and y=0.75B*, are considered for each wedge. As seen, the pressures on the same location are higher when the constant velocity is applied for all the cases. This can be explained by the time history of the impact velocity. Theoretically, the slamming pressure is proportional to the square of impact velocity.

As plotted in Figure 14, the absolute value of the impact velocity is decreasing during the water entry, and the variation is less for a larger deadrise angle, which is the reason that the differences of the pressure histories are smaller when the deadrise angle is 60º as seen in Figure 13 (c).

The results show that the assumption of constant velocity matter the water impact from the point of view of the pressure histories, in particular for the wedge with small deadrise angle. Therefore, it is better to simulate the non-constant impact when the pressure value is concerned.

5.2 CONTACT STIFFNESS

Aquelet et al. (2005) presented the formulation of the penalty coupling algorithm. The penalty stiffness was given in terms of the bulk modulus of the fluid element in the coupling containing the slave structure node, the volume of the fluid element that contains the master fluid node, and the average area of the structure elements connected to the structure node. In present work, the mesh size is 2.5mm, and the penalty factor is set as 0.1, so the numerical stiffness by unit area is 90 *Gpa/m*. With this stiffness, there is no fluid leakage through the structure. Stenius et al. (2006) found that too large contact stiffness could cause numerical noises in the solution. As seen in Figure 10, numerical noises are observed for the deadrise angle 45º. The contact stiffness is one possible reason for this.

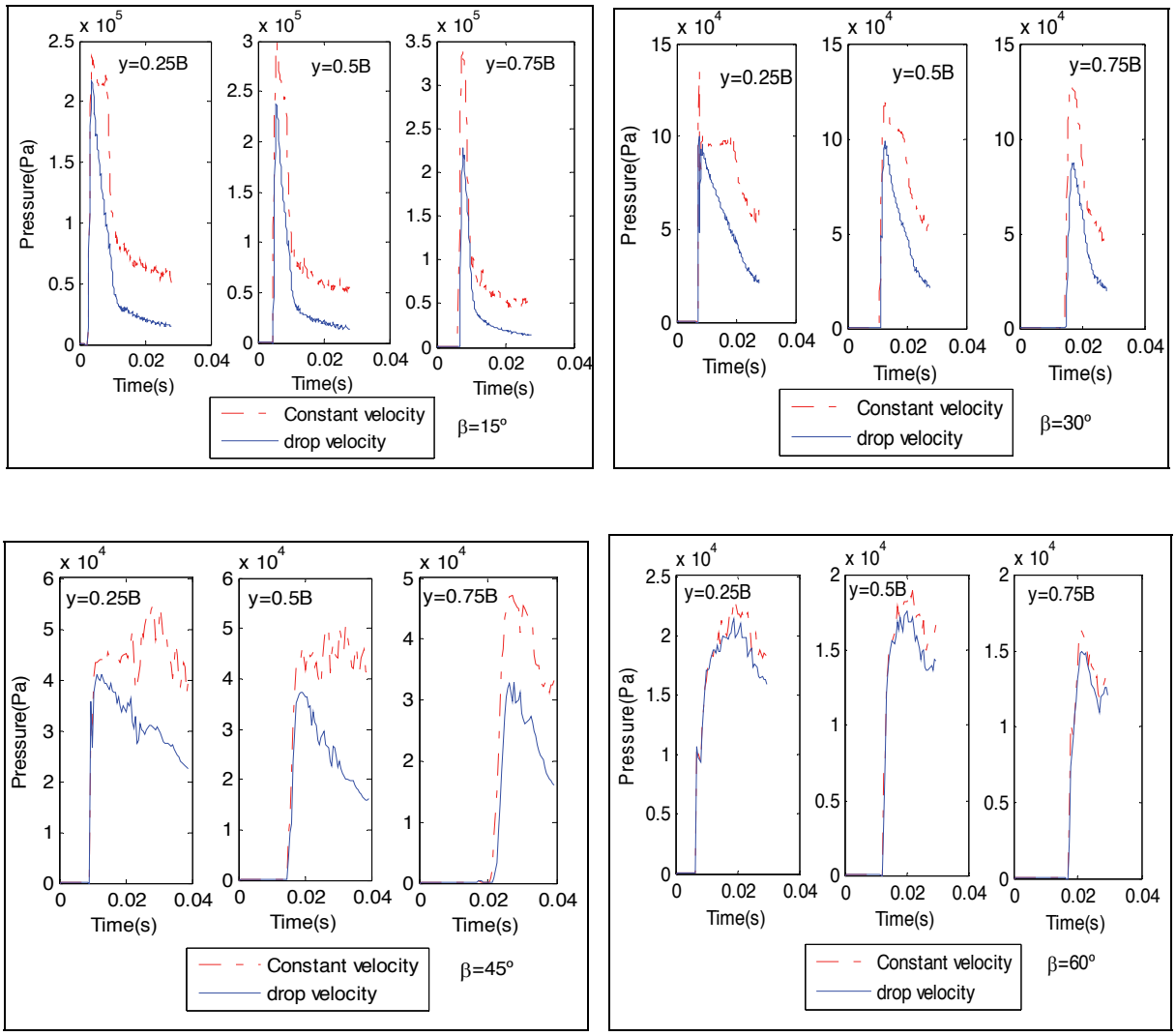

Figure 13. Pressure histories on the wedges entering into water with constant and drop velocity.

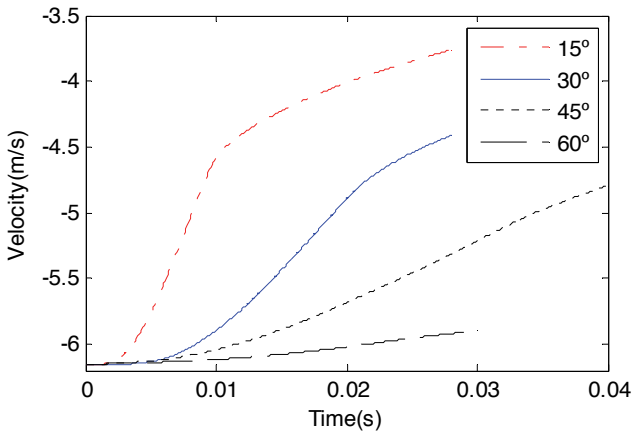

Figure 14. Time history of the impact velocity for the wedge entering into water with drop velocity.

5.3 COMPUTATIONAL TIME

One disadvantage of the explicit finite element method used in this work is the costly computational time. The computational time is mainly related to the minimum mesh size, the number of the elements, the solution time, and the time step factor. An important factor is to reduce the computational time by using these parameters properly.

For all the cases in this work, the minimum mesh size is 2.5mm and the time step factor is set as 0.2 which is the largest value that can prevent the negative volume problem. For the wedge with a deadrise angle 45º, the solution time (0.04s) is the longest one because of the largest size of A. For this case, the computational time is 20 hours 37 min. 50 sec. When the deadrise angle is 10º, the solution time (0.02s) is the shortest one. For this case, the computational time is 7 hours 34 min. 30 sec. All the simulations are conducted on one PC with 2.4 GHz processor and 2 Gigabytes of memory.

6. CONCLUSIONS

Water impact of symmetric wedges with different deadrise angles are analysed by an explicit finite element method. The impact velocity is defined as a constant value -6.15m/s in the vertical direction. The predicted pressure distributions, maximum values of the pressure coefficient, the force coefficient and the vertical impact force are in good agreement with published theoretical and analytical calculations. Some differences exist for small deadrise angles, e.g., 10º, but the differences are not large.

The effects of the deadrise angle are investigated based on the predictions of the wedge with the deadrise angle varying from 10º to 60º. As the deadrise angle increases, the maximum pressure and impact force become smaller. The predicted positions where the maximum pressures happen are somehow lower than other published ones. On the other hand, the effects of the impact velocity are also discussed. As expected, the larger is the velocity, the greater is the pressure on the wetted surface of the rigid wedge.

The evolutions of the pressure distribution and free surface elevations for different deadrise angles are also presented. The results show that the maximum pressure is located near the spray root of the water jet before flow separation, and then it moves towards the keel of the section for a small deadrise angle. When the deadrise angle is close to 45º, the pressure is almost uniformly distributed along the bottom surface before flow separation, and then the maximum value occurs at the keel in the late stage of the impact. For a deadrise angle larger than 60º, the maximum pressure is always located at the keel.

As seen in the comparisons between the predictions in this work and other available calculations, the accuracy of this explicit finite element is achieved for the two-dimensional water impact problem, in particular for the case with medium deadrise angle. On the other hand, the computational time shows the acceptable efficiency as well. Although, the accuracy is not consistent with the deadrise angle of the wedge, the contact stiffness needs to be further study. It can be concluded that this method is effective only if the control parameters are set properly.

It must be noted that, the numerical analysis is not limited to the vertical water entry of symmetric wedges. With proper parameters, it can be applied to analyse the water impact of an arbitrary section with vertical or horizontal velocity, and even three-dimensional problems. However, in these cases the computational time will increase, and the selection of the contact stiffness is more complicated.

7. ACKNOWLEDGEMENTS

The work has been performed in the scope of the project EXTREME SEAS – Design for Ship Safety in Extreme Seas, (www.mar.ist.utl.pt/extremeseas), which has been partially financed by the EU under contract SCP8-GA-2009-234175. Dr Hanbing Luo has been involved in the earlier phases of this research and has contributed to the present understanding on how to deal with the numerical modelling.

8. REFERENCES

1. Aquelet N., Souli, M. and Olovsson, L, Euler–Lagrange coupling with damping effects: Application to slamming problems, *Computer Methods in Applied Mechanics and Engineering*, Volume 195, pp 110-132, 2005.
2. Brizzolara, S., Couty, N.,Hermundstad, O.,Ioan, A., Kukkanen, Timo,Viviani, M., Temarel, P., Comparison of experimental and numerical loads on an impacting bow section, *Ships and Offshore Structures*, Volume 3 (4), pp 305-324, 2008.

3. Das, K. and Batra, R.C. Local water slamming impact on sandwich composite hulls, *Journal of Fluids and Structures*, Volume 27, pp 523-551, 2011.
4. Dobrovol'skaya Z.N., On some problems of similarity flow of fluids with a free surface, *Journal of Fluid Mechanic*, Volume 36, pp 805-829, 1969.
5. Kihara, H., Numerical modeling of flow in water entry of a wedge, *Proc. 19th international workshop on water waves and floating bodies*, CD-ROM, pp 1-4, 2004.
6. Luo, H.B., Wang S., and Guedes Soares C., Numerical prediction of slamming loads on rigid wedge for water entry problem by an explicit finite element method, *Advances in Marine Structures*, Guedes Soares, C, and Fricke, W., (Eds), Taylor & Francis, UK, pp 41-47, 2011.
7. Mei X.M., Liu Y.M, and Dick K.P. Yue, On the water impact of general two-dimensional sections, *Applied Ocean Research*, Volume 21, pp. 1-15, 1999.
8. Ochi, M.K. and Motter, L.E., Prediction of slamming characteristics and hull response for ship design, *Transactions SNAME*, Volume 81, pp. 144-190, 1973.
9. Peseux, B., Gornet, L. and Donguy, B., Hydrodynamic impact: Numerical and experimental investigations, *Journal of Fluids and Structures*, Volume 21(3), pp 277-303, 2005.
10. Ramos, J. and Guedes Soares, C., Vibratory response of ship hulls to wave impact loads, *International Shipbuilding Progress*, Volume 45(441), pp 71-87, 1998.
11. Stavovy, A.B. and Chuang, S.L., Analytical determination of slamming pressures for high speed vessels in waves, *Journal of Ship Research*. Volume 20, pp 190-198, 1976
12. Stenius I., Rosn A. and Kuttenkeuler, J., Explicit FE-modeling of fluid-structure interaction in hull-water impacts, *International Shipbuilding Progress*, Volume 53, pp 1031-121, 2006
13. Von Kármàn, T., *The impact on seaplane floats during landing*. National Advisory Committee for Aeronatics, Techinical note No. 321, pp. 309-313, 1929.
14. Wagner, H., Uber Stossund Gleitvergange an der Oberflache von Flussigkeiten, *Zeitschrift fuer Angewandte Mathematik und Mechanik*, Volume 12, pp 193–215, 1932.
15. Wang, S., Luo, H.B. and Guedes Soares, C., Explicit FE simulation of slamming load on rigid wedge with various deadrise angles during water entry, *Maritime Technology and Engineering*, Guedes Soares, C, et al. (Eds), Taylor & Francis, UK, pp. 399-406, 2012.
16. Wang, S., Assessment of slam induced loads on two dimensional wedges and ship sections, Master thesis on Naval Architecture and Marine Engineering, Instituto Superior Técnico, Technical University of Lisbon, Portugal, 2012.
17. Zhao, R. and Faltinsen O.M., Water Entry of Two-Dimensional Bodies, *Journal of Fluid Mechanics,* Volume 246, pp 593-612, 1993.
18. Zhao R., Faltinsen O.M. and Aarsnes J.V., Water entry of arbitrary two-dimensional sections with and without flow separation, *Proc. 21st Symposium on Naval Hydrodynamics, pp 408-423*, 1996.

